Neutral depletion and beam defocusing in harmonic generation from strongly ionized media

M. Bellini,[1,2] C. Corsi,[2] and M. C. Gambino[3]
[1]*Istituto Nazionale di Ottica Applicata, Largo Enrico Fermi, 6, I-50125 Florence, Italy*
[2]*European Laboratory for Non-Linear Spectroscopy (LENS) and INFM, Largo Enrico Fermi, 2, I-50125 Florence, Italy*
[3]*Department of Physics, University of Florence, Largo Enrico Fermi, 2, I-50125 Florence, Italy*
(Received 16 November 2000; revised manuscript received 21 March 2001; published 5 July 2001)

We present a detailed experimental study of the effects of strong ionization in the process of medium-order harmonic generation. The intensity-dependent density of free electrons significantly modifies the conversion efficiency due to the combined effect of depletion of the neutral atoms and defocusing of the pump beam. We find that the harmonic yield is maximized for particular values of the pump-laser intensity and that, for the range of experimental parameters we used, such optimum intensities do not depend on the harmonic order or on the focusing geometry, but only on the ionization potential of the gas. Finally we show how the defocusing due to ionization is effective in guiding the pump beam along channels of optimum intensity, thus enhancing the overall conversion efficiency for particular focusing conditions. A simple model is presented that, though relying on very crude approximations of the processes at play, is nevertheless able to reproduce the experimental results in a surprisingly good way.

DOI: 10.1103/PhysRevA.64.023411 PACS number(s): 42.50.Hz, 32.80.Rm, 42.65.Ky

I. INTRODUCTION

The generation of high-order harmonics is now a well-established method to produce pulsed radiation in the short-wavelength region of the electromagnetic spectrum [1]. By the interaction of short and intense visible laser pulses with the atoms of a supersonic jet, odd-order harmonics of the fundamental laser frequency are generated. Depending on the pulse wavelength and peak intensity and on the ionization potential of the atoms, very high orders can be efficiently generated at wavelengths down to the extreme ultraviolet (XUV) or to the soft x-ray regions.

According to the standard picture of the high-order harmonic generation (HHG) process [2], every half optical cycle of the laser electrons undergo tunneling ionization through the potential barrier formed by the atomic potential and by the electric-field potential of the laser itself; after being accelerated in the ionization continuum by the field, they may come back to the ion core and recombine to emit harmonic photons that release the accumulated kinetic and ionization energy. Simple semiclassical calculations show that the cutoff energy, i.e., the maximum return energy of the electrons (and, correspondingly, the maximum energy of the emitted harmonic photons) is given by $E_{cutoff} \approx I_p + 3.2U_p$, where I_p is the ionization potential of the atom and U_p is the so-called ponderomotive energy, which is proportional to the intensity of the laser field and the wavelength squared.

As seen above, a certain degree of medium ionization is always present and is indeed necessary for HHG to take place. However, besides being a fundamental ingredient for HHG, ionization also poses serious limits to the possibility of extending the generation process toward higher yields and shorter wavelengths by increasing the interaction intensity. When the intensity of the laser reaches the so-called saturation intensity I_s, a significant fraction of the neutrals in the medium has been depleted and the generation process stops unless the intensities at play are so high as to further ionize the produced ions. If $W(I)$ is the ionization rate for the considered atoms and τ is the laser pulse duration, the saturation intensity is accordingly defined as $W(I_s)\tau \equiv 1$. $W(I)$ being a monotonously increasing function of I, higher saturation intensities can be reached with shorter laser pulses and, of course, with light noble gases having higher ionization potentials. The highest harmonic orders generated to date have indeed been produced in helium with pulse durations shorter than 25 fs [3,4].

Besides putting a limit to the maximum useful interaction intensity, the presence of free electrons in the gas also changes the dispersion properties of the medium itself by providing an intensity-dependent index of refraction for the fundamental and the harmonic fields. This effect, especially for high harmonic orders, can introduce a significant phase mismatch between the generated field and the driving nonlinear polarization, and can substantially limit the effective length of coherent interaction in the medium [5].

Moreover, due to the strong spatial and temporal dependence of the intensity profile of the pulses, strong spatial and temporal phase modulations are imparted on the laser field. These, in turn, result in self-defocusing and self-phase modulation of the beam. While the latter can be shown to mainly produce a blueshift on the spectrum of the harmonics [6], the first effect can substantially modify the propagation of the laser beam through the ionized sample [7,8] and affect the conversion efficiency.

With the now commonly available 100 fs, high-repetition rate, milliJoule level, Ti:Sa amplified laser systems, both neutral depletion and beam defocusing can pose a limit to the generation of medium-order harmonics in the vacuum ultraviolet and XUV region. Such relatively low harmonic orders are the most interesting for the extension of high-resolution spectroscopic studies of atoms, molecules, and ions to the short-wavelength regime [9].

In order to increase the laser peak intensity available in the focus (to improve the harmonic yield) and to decrease it

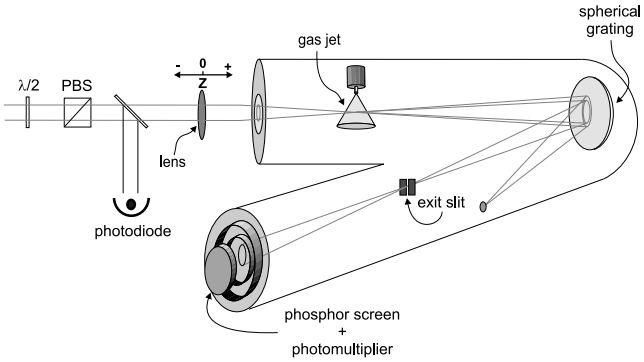

FIG. 1. Experimental setup.

on the monochromator grating (not to damage it), relatively high numerical apertures are normally used in these situations, with confocal parameters of the laser beam comparable to the length of the gas jet. Heavy (and easy to ionize) noble gases are often chosen as the generating medium in this wavelength range thanks to their higher conversion efficiency.

In this paper we study in a detailed way the effects of strongly ionized, heavy noble gases (argon and xenon) on the generation efficiency of such medium-order harmonics.

We show that only the ''geometrical'' effects of medium ionization seem to play a significant role in these situations, determining the conditions for best harmonic conversion.

By changing both the laser-pulse energy and the relative position between the gas jet and the laser focus, we find that the positions of maximum efficiency follow contour lines of constant intensity and that this is closely related to the saturation intensity of the gas.

An extremely simple model is introduced that seems to fully explain the observed behavior. By noting that the observed features do not depend on the harmonic order but only on the ionization potential of the gas, we also find that, in these experimental conditions, the main contribution to the conversion efficiency dependence on the focus-jet position is not given by phase-matching effects but by the depletion of the neutral medium.

The observed asymmetries in the efficiency plots are explained as the result of defocusing of the pump beam due to the presence of free electrons. While in most cases this can reduce the overall efficiency, we find that in some conditions it can actually enhance it by forming channels of almost constant optimum intensity. Also in this case, we are able to reproduce in a good qualitative way all the experimental results by means of our simple model. Other peculiar features, such as the strongly nonmonotonous dependence of the harmonic yield on the pump-laser intensity under particular experimental conditions, can be clearly explained and are well reproduced by our simulations.

II. EXPERIMENT

The experimental setup is sketched in Fig. 1 and is composed of a vacuum chamber equipped with an electromagnetic valve for the interaction between the laser pulses and the gas jet, and a vacuum, 1 m, normal-incidence monochromator for the spectral selection of the different harmonic orders produced. The Ti:Sa amplified laser system provides 0.7-mJ, 100-fs pulses centered around 800 nm and with a 1-kHz repetition rate. Due to the limitations connected to the valve and to the pumping system used to evacuate the monochromator, the rate of gas injection in the chamber is generally kept to a lower value, around 100 Hz. Xenon and argon have been used for the experiments at a constant backing pressure of about 1.5 bar.

Two lenses, of 150 and 200-mm focal lengths have been used to focus the laser pulses inside the interaction chamber. The distance between the laser focus and the gas jet has been varied by moving the lenses along the propagation direction defined as z by means of a translation stage. By defining the position $z=0$ as the location of the gas jet, positive values of z mean that the laser is focused beyond the jet and that the beam interacts with the atoms while converging towards the waist. On the other hand, negative values of z mean that the waist is before the jet and that the beam is diverging when it encounters the atoms.

A preliminary set of measurements has been devoted to the study of the beam size in the vicinity of the focus. A charge coupled device camera has been used to acquire images of the laser beam in planes perpendicular to the direction of propagation; the waist radii at $1/e^2$ along x and y, $w_x(z)$ and $w_y(z)$, have been extracted from the data and the area of the beam has been calculated as $S(z)=\pi w_x(z)w_y(z)$. A polynomial fit has then been used to model the measured areas as a function of the propagation distance. The effective laser peak intensity has been finally calculated as

$$I(z,P)=\frac{2P}{DS(z)}, \tag{1}$$

where P is the measured average power of the laser, and D is the duty cycle, defined as the product of the pulse duration and pulse repetition rate. The above procedure has been preferred to the simpler assumption of a pure diffraction-limited Gaussian beam because of the known poor spatial homogeneity of our laser. The M^2 factor of the beam has been measured to be of the order of 2, with a minimum beam waist in the focus of about 20 μm for the 200 mm lens. The measured Rayleigh range is about 1.8 mm, which is longer, but still comparable with the estimated length of the gas jet, $L\approx 0.8$ mm.

The monochromator is equipped with a spherical, 600-lines/mm diffraction grating that allows for a spectral resolution of about 0.04 nm when the exit slit is closed to about 10 μm. However, for the measurements discussed here, the exit slit has been kept completely open in order to measure the total, spectrally integrated, harmonic yield, while still being able to easily discriminate between different harmonic orders. This has been done to integrate over the possible blueshifts of the spectra and to compensate the changes in throughput when moving the focus position.

Harmonics have been observed downstream of the exit slit of the monochromator by means of a tetraphenyl buthadiene (TPB) phosphor screen and a photomultiplier. The TPB

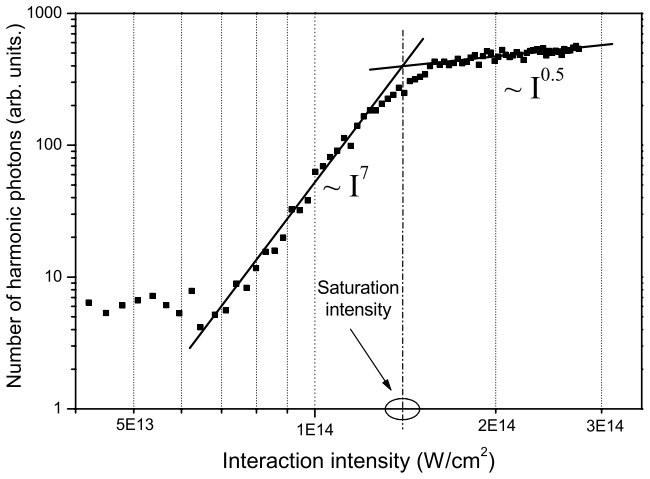

FIG. 2. Yield of the 13th harmonic in xenon as a function of the pump laser intensity. The beam waist produced by a 200 mm focusing lens is placed 2 mm beyond the gas jet. Two regions with very different slopes are evident.

converts the XUV photons into visible (about 400 nm [10]) light pulses, which are then detected by the photocatode. A photodiode, receiving a small fraction of the pump-laser light, has been used to monitor the laser-pulse energy after proper calibration.

All the scans have been performed by first selecting a given relative jet-focus position, and then by recording simultaneously both the harmonic signal and the signal from the photodiode as the pump pulse energy is continuously varied by means of a half-wave plate and a polarizer. Different scans of the relative jet-focus position have been performed in 500 μm steps. All the signals have been acquired by a digital oscilloscope and stored on a personal computer for subsequent processing.

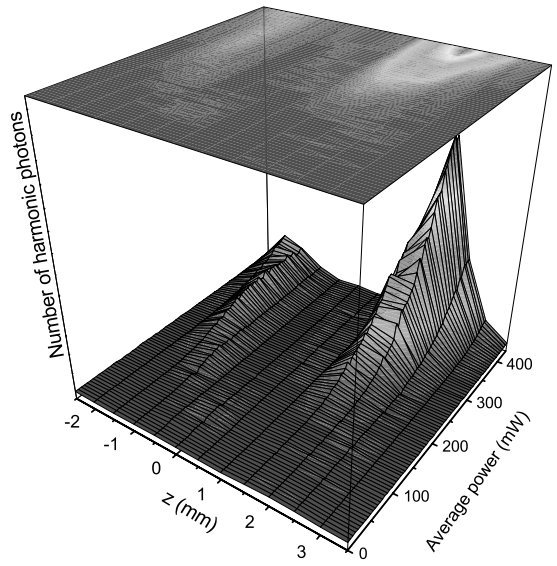

FIG. 3. 3D plot of the measured 13th harmonic yield as a function of the average laser power and of the relative focus-jet distance.

III. RESULTS

A logarithmic plot of the harmonic yield as a function of the interaction laser intensity is shown in Fig. 2 for the 13th harmonic in Xe. The data have been taken for $z=+2$ mm, i.e., with the focus of the laser beyond the gas jet. The curve has a clear exponential behavior with two different growing rates separated by a net knee where the curve drastically changes slope. While the first exponent is of the order of 7, the second part of the curve shows a much slower growth with the laser intensity and the corresponding exponent is about 0.5, meaning that the relationship is now less than linear. Very similar behaviors have been observed for several harmonics in the plateau (we have studied harmonic orders between the 5th and the 19th) and also in the case of argon. The intensities at which the curves change slope are about 1.6×10^{14} W/cm^2 for xenon and 2.8×10^{14} W/cm^2 for argon.

As we will show in the following discussion, this behavior is connected to the depletion of the neutral atoms in the gas, and the intensity where the curves get flatter can be easily estimated.

Figure 3 presents one measured three-dimensional plot which is representative of the general behavior of the overall harmonic yield as a function of the relative focus-jet position and of the laser average power. This plot in particular is relative to the 13th harmonic obtained with a 150 mm focusing lens in Xe, but all the experiments have, however, given the same general trend: a single peak at $z=0$ for low pump power, and a bifurcation into two peaks (almost symmetric around $z=0$ but with quite different heights) for higher incoming powers. The position $z=0$ has been defined experimentally as the position of maximum harmonic yield or maximum visible plasma light (the two methods give identical results) at very low laser powers.

The positions of the most intense right peak, located at $z>0$ (when the laser focuses beyond the gas jet), are also reported in Fig. 4, superposed to the experimental contour plots of the peak laser intensity for various combinations of harmonic orders, focusing lenses, and atomic media.

In all cases, the peaks are located at $z=0$ for low powers and then, after some initial deviations, follow almost exactly contour lines of constant intensity when the power is increased. These intensities do not show a significant dependence on the harmonic order but they clearly depend on the gas used for the generation and are the same with different focusing lenses. The limit intensities found for argon and xenon are again 2.8×10^{14} and 1.6×10^{14} W/cm^2, respectively.

IV. DISCUSSION

A. Depletion effects

Depending on the laser intensity, the creation of free electrons can be described by one of the following models: multiphoton or tunneling ionization. The separation between these regimes is given by the Keldysh constant γ defined by [11]

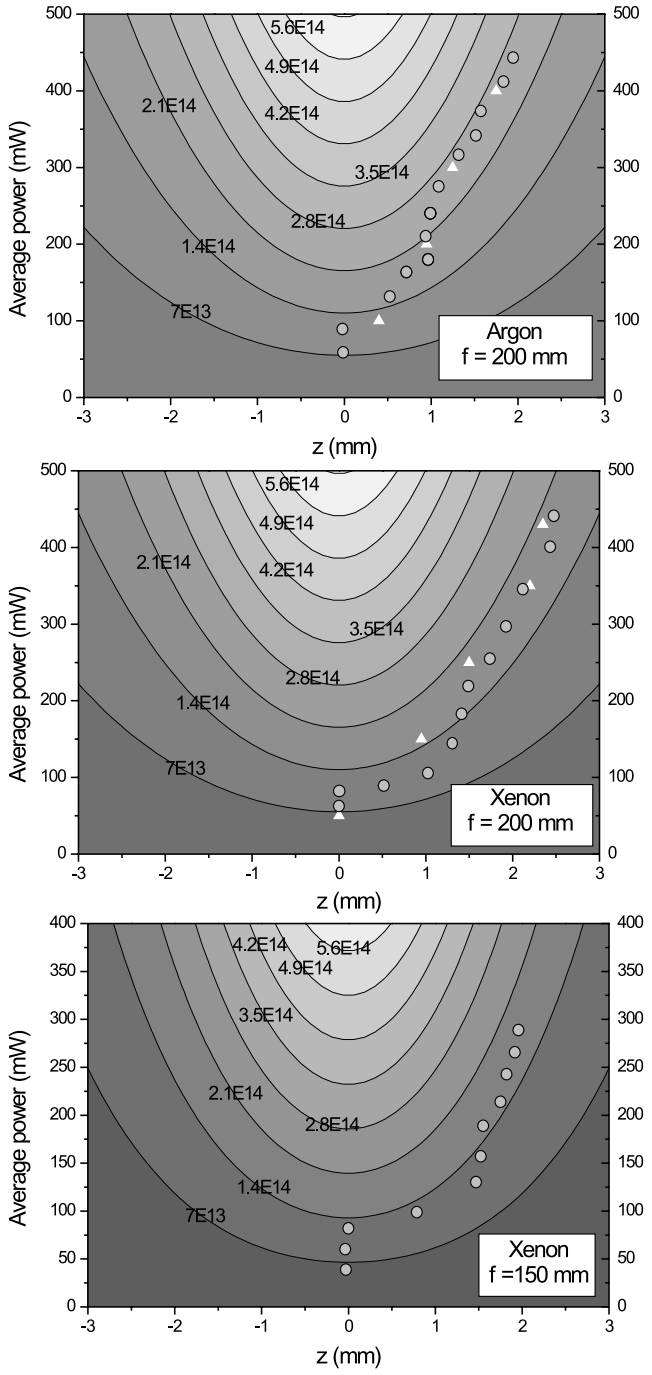

FIG. 4. Positions of the measured peaks in the harmonic conversion efficiency. In the three figures the circular and triangular data points are relative to the 13th and to the 5th harmonics, respectively. The contour lines of equal laser intensity are calculated on the basis of the measured size of the beam around the focal region. Data for the 150-mm lens have been taken by partially blocking the laser beam with an iris; this explains the lower available powers and the similar shape of the contour lines with respect to the case of the 200 mm lens.

$$\gamma = \sqrt{\frac{I_p}{2U_p}}, \tag{2}$$

where I_p is the ionization potential of the atom and U_p is the ponderomotive energy defined above. For $\gamma<1$, the tunneling regime is dominant, whereas for $\gamma>1$ the multiphoton regime is the strongest effect. In the multiphoton perturbative regime the ionization rate is given by

$$W_{mp}(t) = \sigma I(t)^q, \tag{3}$$

where q is the number of photons required to ionize the atom from the ground state. In the tunneling regime the Ammosov-Delone-Krainov [12] model can be used to find the ionization rate:

$$W_{ADK}(t) = \sqrt{\frac{3E}{\pi E^*}} |C_n|^2 \left(\frac{2E^*}{E}\right)^{2n-1} I_p \exp\left(-\frac{2E^*}{3E}\right), \tag{4}$$

where E is the field amplitude, $E^* = (2I_p)^{3/2}$, C_n is a numeric constant of the order of 2 and $n = Z(2I_p)^{-1/2}$, with Z the residual ion charge. In order to quantify the ionization effect, we use a ''hybrid'' model that combines the multiphoton and the tunneling models. The value of σ in Eq. (3) is then fixed by equating the multiphoton and the tunneling rate for $\gamma = 1$.

In the gaseous medium, the temporal change in the electron density $N_e(t)$ at time t is described by the rate equation

$$dN_e(t) = N(t) W(t) dt, \tag{5}$$

where $N(t)$ is the neutral atom density and $W(t)$ is the ''hybrid'' ionization rate depending on the field amplitude at time t. If we only consider singly ionized species, then $N_0 = N_e(t) + N(t)$, where N_0 is the initial density of the neutral atoms. From Eq. (5), $N(t)$ can be found to decrease in a laser pulse as

$$N(t) = N_0 \exp\left[-\int_{-\infty}^{t} W(t')dt'\right]. \tag{6}$$

Here we also use an alternative definition of the saturation intensity I_s for a given gas as the minimum laser peak intensity for which the neutrals have been completely depleted at the end of the pulse. This can be operatively defined as

$$\left.\frac{N(\infty)}{N_0}\right|_{I_0 = I_s} \equiv 0.001. \tag{7}$$

With the above definition, the saturation intensities for an 800 nm, 100 fs FWHM, Gaussian pulse are $I_s(\mathrm{Xe}) = 1.5 \times 10^{14}$ W/cm^2 and $I_s(\mathrm{Ar}) = 3.5 \times 10^{14}$ W/cm^2.

Considering the residual uncertainties in the experimental intensity determination, these values are in a pretty good agreement with the measured location of the knee in the harmonic yield curves shown in Fig. 2. We can then assume that the general trend is that of a fast exponential growth when the laser intensity is lower than the saturation level and an almost constant or just slightly increasing harmonic yield when the medium is completely ionized above I_s. The residual increase above I_s may be due to harmonic generation by ionized atoms or, more likely, to the fact that we are

dealing with a bell-shaped beam and, while in the center of the beam the ionization of the gas is already complete, it can still go on in the wings of the transverse spatial distribution.

Clearly, when the relative position between the laser focus and the gas jet is varied, similar curves should be found, with the knees located at the same value of laser intensity but now corresponding to quite different pulse energies. Approaching $z=0$, a low power is in fact needed to saturate the yield, due to the small beam size close to the focus; conversely, when $|z|$ gets larger and the focus is moved away from the jet, saturation can only take place for high enough laser powers.

A further effect of changing the focus-jet relative position is, however, to be considered, if we assume that harmonic emission is only limited by the medium length and that the gas pressure in the jet is constant, then the final number of harmonic photons, scales linearly with the transverse section $S(z)$ and quadratically with the interaction length L. It can thus be modeled as

$$N_h(z,P) \propto f(I(z,P))S(z)L^2 \tag{8}$$

where $I(z,P)$ is given in Eq. (1) and the function $f(I(z,P))$ is defined as

$$f(I(z,P)) = \begin{cases} I(z,P)^p & \text{if } I(z,P) < I_s, \\ \dfrac{I_s^p}{I_s^s} I(z,P)^s & \text{if } I(z,P) \geqslant I_s \end{cases} \tag{9}$$

in order to model the experimentally found behavior shown in Fig. 2. The parameter p is the exponent in the nonsaturated regime, while s is the exponent for the situation where saturation is present. Though these assumptions are a very crude approximation of the real situation, we will show that they can model the experimental observations in a surprisingly good way.

If we keep the average laser power P constant, the first two factors in Eq. (8) depend on the beam waist size at position z. For large values of $|z|$ (i.e., far from the focus) the waist is large and the laser intensity is lower than the saturation intensity. In these conditions, it is convenient to decrease $|z|$, as the effect of a smaller interaction volume is overcompensated by the rapid exponential growth of the harmonic yield with increasing laser intensity. However, when $|z|$ is so small that the laser intensity reaches saturation, the harmonic yield almost stops growing with the pump intensity and the main contribution now comes from the decreasing interacting volume: going towards the focus only has the result of diminishing the number of atoms available for harmonic generation.

It is evident that the overall dependence of $N_h(z,P)$ on z at a constant value of P shows a symmetric double peak centered around $z=\pm z_s(P)$, where $z_s(P)$ is the position along the propagation axis where the pulse reaches the saturation intensity. Using a Gaussian beam with a peak intensity of I_0 and a waist w_0 in the focus, these points are easily found as

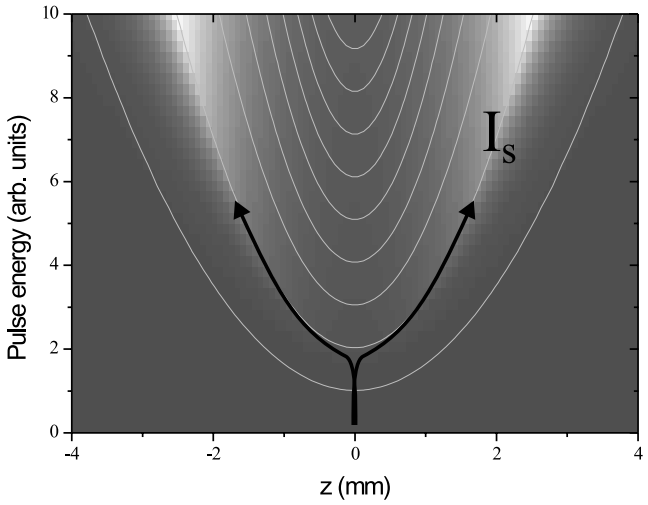

FIG. 5. Map of calculated harmonic intensities. The solid arrows indicate the predicted locations of maxima in the harmonic yield.

$$z_s(P) = \frac{\pi w_0^2}{\lambda} \sqrt{\frac{I_0(P)}{I_s} - 1}. \tag{10}$$

Of course, when the pulse energy is so low that, even at the focus, I_0 is lower than the saturation intensity, then the above equation has no real solution and the curve shows a single central peak at $z=0$. So, as expected, for low pulse energies, the best conversion efficiency is obtained by placing the laser focus directly below the gas jet.

In Fig. 5 we show a plot of the calculated laser and harmonic intensity as a function of both the z position and the energy of the incoming pulses; the harmonic intensity values are given as a gray-scale density plot, while a contour plot shows the different laser intensities. For simplicity, the waist size in this case has been determined from the formulas for a pure Gaussian beam propagation and not from the real experimental data; the exponents p and s used to calculate the data are those found experimentally.

Starting from low pulse energies, a single maximum is encountered until the intensity in the focus reaches the saturation value; from that point on, the peaks for harmonic conversion move away from the focus and diverge with increasing energy. It should be noted that the same qualitative behavior can be found for a wide range of exponents p and s; the locations of maxima keep following the contour lines corresponding to $I(z,P)=I_s$ as long as $p>2$ and $s<2$.

Structures with multiple maxima of the harmonic conversion efficiency as a function of z have been predicted and observed by several authors in a range of different experimental conditions and have been often interpreted as effects related to the phase matching between the pump and the harmonic field [13–17]. Such factors, closely related to the phase shift induced by focusing, to the atomic dipole phase, and to the phase mismatch induced by plasma dispersion, are strongly dependent on the harmonic order and start to limit the conversion efficiency only for sufficiently high harmonics.

Moreover, according to experimental observations [17] and theoretical predictions [15,16], the conditions that en-

hance phase-matching on-axis in the presence of geometrical and intensity-induced dipole phase shifts, are those where the gas jet is placed in the divergent part of the focused laser beam or, with our conventions, for $z<0$. The fact that in all our measurements the situation is always reversed, with the peak at $z>0$ much more intense than the other, shows that we are working in quite different experimental conditions. In particular, in most of the theoretical works, the medium ionization was absent or completely neglected while, as we have seen, it plays a relevant role in our case. Indeed, the conditions for maximum harmonic conversion correspond to the saturation intensities defined above and the gas is always almost fully ionized at these points; furthermore, we observe the full angular spread of the harmonic beams, so that off-axis emission also contributes significantly. In the case of the experimental work of Ref. [17], though ionization was substantial, the harmonic yield was measured by aperturing the XUV beam with a pinhole, thus essentially observing only the photons emitted on axis, where phase-matching effects were still evident.

The fact that in our experimental conditions only the ionization potential of the gas seems to determine the optimum intensity for harmonic generation, independently from the order, strongly supports the assumption that phase matching does not limit harmonic conversion in this case. This might look puzzling, especially considering the fact that at the saturation intensity and with the gas densities used in our experiment, one should at least expect a substantial phase mismatch due to free-electron dispersion, especially for the higher harmonic orders considered. In particular, one finds that, already for the 13th harmonic, a fully ionized gas results in a coherence length of about 250 μm, significantly shorter than the length of the medium itself.

A possible explanation is the following: while we have found that the best geometrical conditions (to ensure that the maximum interaction volume is achieved at the maximum useful intensity) are those where all the atoms have been ionized by the end of the pulse (i.e., when the peak pulse intensity equals I_s), this does not imply that the harmonic pulses are really generated at such instantaneous intensity. Indeed, our relatively low-order harmonics require a much lower laser intensity for generation and are mostly produced quite early in the leading edge of the pulse. At such times ionization is still far from complete and the dephasing suffered by the pulses propagating ahead of the main ionization front is not high enough to limit the interaction length. A deeper experimental investigation of the times of production and of the effective generating intensities and ionization levels for different harmonic orders has also been carried out in the frame of the present work and will be the subject of a forthcoming paper.

B. Defocusing effects

The strong asymmetry in the heights of the left and right peaks is connected to the defocusing induced by free electrons on the fundamental laser field. Such defocusing is due to the refraction of the laser beam propagating through the spatially modulated plasma created by the leading edge of the pulse itself. It has been shown that this self-defocusing can limit the laser intensity achievable in the ionizing medium to a value much lower than I_0 and can substantially modify the propagation of the laser beam [7,8]. The effect of laser beam defocusing on harmonic generation has already been pointed out in Refs. [18–20] and it has been analyzed in some more detail by Miyazaki *et al.* in Refs. [21,22]. These two works, in particular, concentrate on several effects of ionizing media on the process of harmonic generation and succeed in giving a convincing explanation of the observed behaviors. The authors show that the asymmetries in the harmonic yield as a function of the focus position, are essentially due to the defocusing of the fundamental beam, and give strong qualitative arguments to support their assumptions. However, a full quantitative model to describe these effects is not developed and the authors do not try to reproduce their experimental results with calculations, so that the possibility of making predictions for different experimental conditions appears limited.

Here we concentrate on the same geometrical effects of ionization, but we give some general relationships that may allow to relate all the observed structures to the experimental parameters in a simple way. To this purpose we introduce a model to take the effects of beam defocusing into account and compare the results of simulations based on this simple model with the data that we have obtained under quite various experimental conditions.

We can start by recalling that the refractive index of the ionized medium can be expressed as

$$n=\sqrt{1-\frac{\omega_p^2}{\omega^2}} \tag{11}$$

$$=\sqrt{1-\frac{N_e}{N_c}}, \tag{12}$$

where ω is the frequency of the laser and the plasma frequency ω_p is defined as

$$\omega_p^2=\frac{N_e e^2}{m\varepsilon_0}. \tag{13}$$

N_e is the electron density and N_c is the critical density given by

$$N_c=\frac{m\varepsilon_0\omega^2}{e^2}. \tag{14}$$

In the above formulas, m and e are, respectively, the electron mass and charge, and ε_0 is the vacuum dielectric constant. In the case of our laser at 800 nm the critical density is about 1.75×10^{21} cm^{-3}. If N_e is much less than N_c, as in our case, we can express the phase shift suffered on axis by the laser beam after passing through a length L of ionized medium as

$$\Delta\phi_e=-\frac{\pi L}{\lambda}\frac{N_e}{N_c}. \tag{15}$$

This means that the phase of the central ray of the beam is advancing with respect to the phase of off-axis points (where we may consider the electron density neligible). The beam acquires a positive wavefront curvature and will tend to diverge. Of course this phase shift (or wavefront curvature) has to be compared to that intrinsic to a focused Gaussian beam, and the two contributions have to be summed together to give the overall behavior of the beam. The on-axis phase of a Gaussian beam relative to the the plane wave at the same z is simply expressed as

$$\Delta\phi_G = \frac{z}{z_R}, \tag{16}$$

where $z_R = \pi\omega_0^2/\lambda$ is the Rayleigh range of the beam. Clearly this means that the beam is converging ($\Delta\phi_G > 0$) for $z > 0$ and diverging ($\Delta\phi_G < 0$) for $z < 0$. Note that we are still using our modified definition of the variable z, with the laser beam propagating from the right to the left, towards negative values of z.

The total on-axis phase for each (z,P) point in the relative focus-jet position and pulse-peak-power space, is then given by

$$\Delta\phi(z,P) = \frac{z}{z_R} - \frac{\pi L}{\lambda}\frac{N_e(z,P)}{N_c} \tag{17}$$

With these simple assumptions we can immediately explain the asymmetry between the left and right peaks in Fig. 3. When $z > 0$, the two terms in Eq. (17) have opposite signs and tend to compensate each other, while for $z < 0$ they add their contributions to a large negative on-axis phase. In other words, when we place the ionized medium in the converging part of the focused beam, it acts as a divergent lens that tends to collimate it and to maintain the interaction intensity at the optimum value throughout the gas sample. If, on the other hand, the gas jet is placed downstream of the focus, it further increases the divergence of the beam, causing a drop in the intensity and effectively limiting the length of interaction with the gas.

Miyazaki *et al.* found that this is the general rule for lower-order harmonics, that do not need high interaction intensities and are effectively optimized by maximizing the interaction volume at $z > 0$ with the help of the ionization-induced defocusing. Higher-order harmonics, on the other hand, were shown to benefit from the higher intensities available when the gas jet is placed downstream of the laser focus. For harmonics in or near the cutoff, a short-length, high-intensity interaction at $z < 0$ is clearly preferable to a longer path in the collimated beam at $z > 0$ with an intensity that is, however, not sufficient for harmonic generation.

In the present paper we have concentrated on relatively low-order harmonics that are well into the plateau at the saturation intensity of the laser; in this case we are always in the first of the above-described situations and we only observe the dominant peak at positive z values.

We can be more quantitative in the description of our model by noting that, as we have shown before, the peaks are located at $\pm z_s$, where the laser reaches the saturation intensity and the medium gets fully ionized at the end of the pulse. At these points we may then assume that $N_e(z_s,P) \approx N_0$, and we can easily calculate the total on-axis phase. With a medium length $L \approx 0.8$ mm and an estimated gas density $N_0 \approx 4.2\times 10^{17}$ cm^{-3} (corresponding to a pressure in the jet of about 12 Torr), the electronic contribution to the phase is $\Delta\phi_e \approx -0.8$ rad; this value is to be compared to the intrinsic geometric phase $\Delta\phi_G = z_s/z_R$ at the same position. Considering the case of argon with the 200 mm lens (see Fig. 4), the peak positions are located at $z_s \approx \pm 2$ mm for the maximum laser pulse energy; here the corresponding phases are about ± 1.1 rad, with the plus sign corresponding to $z_s = +2$ mm and the minus sign to $z_s = -2$ mm. So, in the first case, the two phase terms almost cancel each other, collimating the beam and forming a new waist close to this position, while in the second case the divergence of the beam practically doubles, causing a sudden drop in the available interaction intensity.

We can assume that placing the ionized medium at a position z along the propagation direction of the unperturbed Gaussian beam, transforms it into another Gaussian beam with different parameters. In particular, both the new position and size of the waist will be different and given by

$$z_{new}(z,P) = \frac{\pi w(z)^2}{\lambda}\frac{\Delta\phi(z,P)}{1+\Delta\phi(z,P)^2} \tag{18}$$

and

$$w_{0new}(z,P) = \frac{w(z)}{\sqrt{1+\Delta\phi(z,P)^2}} \tag{19}$$

where $w(z)$ is the original beam size at position z.

Clearly, when the total phase $\Delta\phi(z,P)$ cancels, a new waist is formed at that position ($z_{new} = 0$) with a new, and larger, size [$w_{0new} = w(z)$]. When, on the other hand, ionization is negligible, the phase on axis tends to the geometrical phase and the two quantities above reduce to the unperturbed values, z and w_0.

From Eqs. (18) and (19) we can now find the new beam divergence at the exit of the ionized gas medium as

$$\theta_{new}(z,P) = -\frac{\lambda\Delta\phi(z,P)}{\pi w(z)}. \tag{20}$$

If we define the effective interaction length with the medium as that over which the relative intensity variations are less than η, we obtain

$$L_{\text{eff}}(z,P) = \frac{\eta w(z)}{2|\theta_{new}(z,P)|}. \tag{21}$$

Of course $L_{\text{eff}}(z,P)$ cannot exceed the length of the medium itself and must be upper-limited to L. The above formula is another crude approximation and is strictly valid only in a region close to the new focus position, but we have nevertheless found that, even at longer distances, it does not deviate much from more accurate estimations and has the great advantage of a very simple analytical expression.

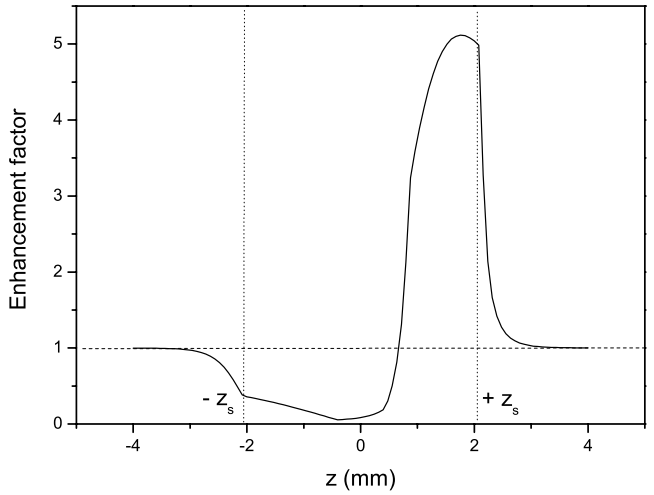

FIG. 6. Plot of the calculated enhancement factor for the harmonic yield in the presence of strong ionization-induced defocusing.

We can now combine Eqs. (21) and (8) to find the total harmonic yield as a function of z and P in the presence of ionization-induced defocusing:

$$N_h(z,P) \propto f(I(z,P))S(z)L^2\left(\frac{L_{eff}(z,P)}{L_{eff}(z,0)}\right)^2. \qquad (22)$$

The last term is a scaling factor that we introduce to keep the defocusing effects into account. A plot of this term as a function of the jet position relative to the laser focus is shown in Fig. 6 for the same experimental conditions of the above example (argon atoms, 200 mm lens and about 450 mW of average input power) and for $\eta = 20\%$. It clearly shows that in $z = +z_s$, the interaction with the whole length of the gas jet enhances the harmonic yield by a factor of about 5, while in the symmetric position, defocusing shortens the effective interaction length and the yield drops to about 30% of its unperturbed value. Note that, as it should be, this scaling factor does not modify the calculated yield for low-ionization conditions, i.e., for low powers or long distances from the focus.

In Fig. 7 we show the measured and calculated 13th harmonic yield in argon as a function of z at fixed laser input power. The two calculated peaks can now well reproduce the experimental asymmetry and both the positions, shapes, and relative intensities of the two maxima are fairly well matched.

The effect of the strong defocusing of the beam due to the presence of free electrons is also evident in other peculiar behaviors that we observed while increasing the laser-pulse energy in $z = 0$. When the laser focus is placed right under the gas nozzle, the harmonic intensity first grows exponentially for low pump powers, then reaches a maximum and finally drastically drops for laser intensities close to I_s. After this region, the yield starts growing again at the slow rate typical of the saturated regime.

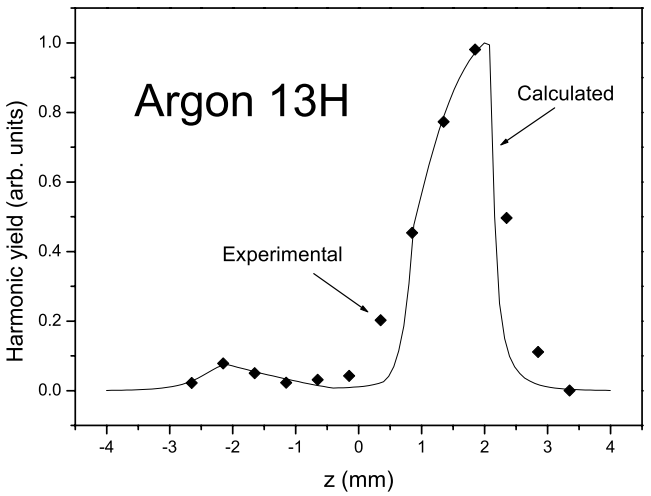

FIG. 7. Experimental and calculated profiles of harmonic yield in argon as a function of the focus-jet relative position at a fixed laser-pulse energy. The defocusing induced by free electrons improves the conversion efficiency when the gas jet is located before the laser focus ($z > 0$) and strongly suppresses it for $z < 0$.

This behavior, which is illustrated in Fig. 8 for xenon atoms with the 150 mm lens, is rather unusual and was not observed in Refs. [21,22], where the harmonic yield at $z = 0$ was always monotonous and was only seen to saturate at higher pump intensities. However, our results can be simply understood as follows: at low pump intensities the harmonic yield grows exponentially until the ionization at the center of the beam is so large as to significantly defocus the laser and decrease the effective length of interaction with the gas to fractions of the full medium length. Here the harmonic yield is reduced to less than 50% compared to the peak value. Note that, before the full ionization limit is reached, the harmonic yield in the absence of defocusing, keeps increasing exponentially in our model, and this partially compensates for the sudden drop [proportional to $(L_{eff}/L)^2$] caused by the interaction length, that might otherwise reduce harmonic emission even more abruptly at these intensities.

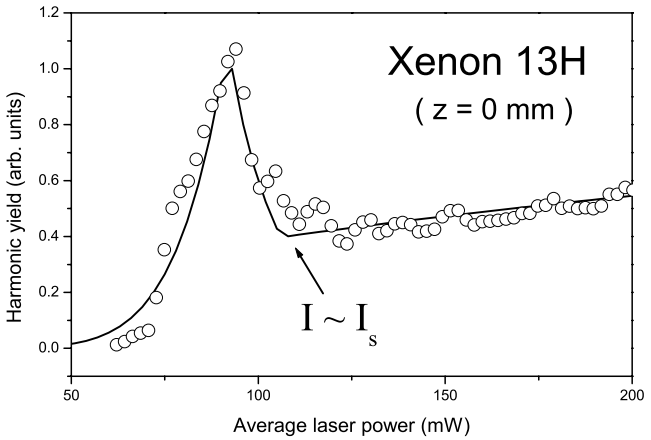

FIG. 8. Measured and calculated yield of the 13th harmonic in xenon as a function of the laser pump power in the presence of strong ionization-induced defocusing. The laser focus produced by a 150 mm focal-length lens is placed directly below the gas nozzle.

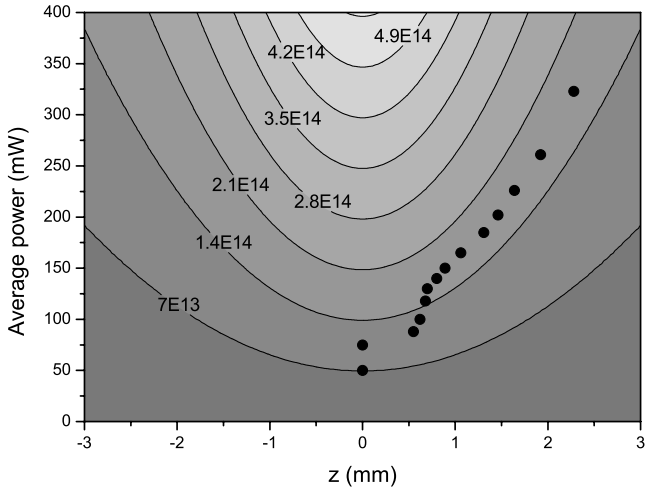

FIG. 9. Calculated positions of the harmonic-yield peaks for xenon and for a 200 mm focusing lens. The situation is the same of the middle plot of Fig. 4.

When the saturation intensity is finally reached, the gas is fully ionized and the defocusing effect saturates to give the minimum interaction volume; increasing the intensity from this situation does not further increase the defocusing and the slow growth of the saturation regime takes over.

One can also use Eq. (22) to calculate the predicted locations of maximum harmonic yield and compare them with the experimental findings. Figure 9 shows these calculated points superposed to the isointensity lines of the laser in the case of xenon with the 200 mm lens; such a plot should be compared with the corresponding situation illustrated in Fig. 4. The maxima keep following lines of constant laser intensity for high enough incident powers, while they start to deviate substantially towards zones of lower intensities when the laser power is reduced. This is in good qualitative agreement with the experimental data and is a further indication of the usefulness of the model.

It should be emphasized that the calculated curves in Figs. 7, 8, and 9 are not best fits to the data but have been directly obtained from Eq. (22) using only the experimentally available parameters. The only remaining arbitrariness is in the parameter η used in the definition of the effective interaction length, but we have found that a single value of $\eta \approx 20\%$ is able to reproduce well all the measured data, regardless of the different experimental situations.

Of course, the agreement between measured and calculated data is not perfect but, keeping in mind the crude assumptions used and the intrinsic discontinuities present in our model, it is surprising to find that it is possible to reproduce the experimental results so well.

V. CONCLUSIONS

In conclusion, we have shown that the process of high-order harmonic generation in strongly ionized media can be well understood and its properties can be accurately predicted on the basis of a simple model. For the intensities and the harmonic orders considered here, the only important contribution to the harmonic yield arises from the combined effect of neutral medium depletion and defocusing of the pump-laser beam.

The depletion of the neutral atoms in the gas jet is responsible for the existence of an optimum laser intensity value where harmonics are generated with the maximum efficiency. We have shown that this value is closely related to the saturation intensity of the gas while it does not seem to depend on the harmonic order, ruling out other possible explanations based on the phase matching with the pump beam.

The defocusing of the laser beam due to the presence of free electrons has been found to be responsible for the strong asymmetries between the two otherwise symmetric conditions of the ''jet before the focus'' and the ''jet beyond the focus.'' The observation that the harmonic yield is maximized when the gas jet is placed in the converging laser beam, shows that ionization is here playing a major role and that it can actually enhance the harmonic conversion by guiding the laser pulse along ''channels'' of constant optimum intensity. This result is contrary to several previous observations and predictions and shows once again that it is ionization and not phase matching that is mainly responsible for the observed behaviors in this regime.

We believe that these experimental results and the simple model introduced to explain them will be of use for the efficient production of medium-order harmonics with the systems now widely available in laboratories around the world. Such laser systems of moderate peak intensity and not-too-short pulse duration are nevertheless very good for the generation of these harmonic orders and are the best candidates for most of the foreseen applications of this new source of coherent radiation.

ACKNOWLEDGMENTS

This work has been carried out at LENS, with the support of the Italian MURST and of the European Community Contract No. ERB FMGE CT 950017.

[1] See contributions in *Applications of High Field and Short Wavelength Sources VII*, Vol. 7 of 1997 OSA Technical Digest Series (Optical Society of America, Washington, DC, 1997).

[2] P. B. Corkum, Phys. Rev. Lett. **71**, 1994 (1993).

[3] Z. Chang, A. Rundquist, H. Wang, M. Murnane, and H. C. Kapteyn, Phys. Rev. Lett. **79**, 2967 (1997).

[4] Ch. Spielmann, N. H. Burnett, S. Sartania, R. Koppitsch, M. Schnürer, C. Kan, M. Lenzner, P. Wobrauschek, and F. Krausz, Science **278**, 661 (1997).

[5] A. L'Huillier, X. F. Li, and L. A. Lompré, J. Opt. Soc. Am. B **7**, 527 (1990).

[6] C.-G. Wahlström, J. Larsson, A. Persson, T. Starczewski, S. Svanberg, P. Salières, P. Balcou, and A. L'Huillier, Phys. Rev. A **48**, 4709 (1993).

[7] P. Monot, T. Auguste, L. A. Lompré, G. Mainfary, and C. Manus, J. Opt. Soc. Am. B **9**, 1579 (1992).
[8] R. Rankin, C. E. Capjack, N. H. Burnett, and P. B. Corkum, Opt. Lett. **16**, 835 (1991).
[9] M. Bellini, S. Cavalieri, C. Corsi, and M. Materazzi, Opt. Lett. (to be published).
[10] G. Naletto, E. Pace, L. Placentino, and G. Tondello, Proc. SPIE **2519**, 31 (1995).
[11] L. V. Keldysh, Zh. Éksp. Teor. Fiz. **47**, 1945 (1964) [Zh. Eksp. Teor. Fiz. **20**, 1307 (1965)].
[12] M. V. Ammosov, N. B. Delone, and V. P. Krainov, Zh. Éksp. Teor. Fiz. **91**, 2008 (1986) [Sov. Phys. JETP **64**, 1191 (1986)].
[13] A. L'Huillier and P. Balcou, Phys. Rev. Lett. **70**, 774 (1993).
[14] P. Balcou and A. L'Huillier, Phys. Rev. A **47**, 1447 (1993).
[15] P. Salières, A. L'Huillier, and M. Lewenstein, Phys. Rev. Lett. **74**, 3776 (1995).
[16] M. Lewenstein, P. Salières, and A. L'Huillier, Phys. Rev. A **52**, 4747 (1995).
[17] A. Bouhal, P. Salières, P. Breger, P. Agostini, G. Hamoniaux, A. Mysyrowicz, A. Antonetti, R. Constantinescu, and H. G. Muller, Phys. Rev. A **58**, 389 (1998).
[18] S. C. Rae, Opt. Commun. **97**, 25 (1993).
[19] S. C. Rae, K. Burnett, and J. Cooper, Phys. Rev. A **50**, 3438 (1994).
[20] C. Altucci, T. Starczewski, E. Mevel, C.-G. Wahlström, B. Carré, and A. L'Huillier, J. Opt. Soc. Am. B **13**, 148 (1996).
[21] H. Sakai and K. Miyazaki, Phys. Rev. A **50**, 4204 (1994).
[22] K. Miyazaki and H. Takada, Phys. Rev. A **52**, 3007 (1995).